J. Plasma Fusion Res. SERIES, Vol. 3 (2000) 140–144

Progress Toward Long Pulse, High Performance Plasmas in the DIII-D Tokamak

POLITZER Peter A.*, LUCE Timothy C., AUSTIN Max E.[1], FERRON John R., GAROFALO Andrea M.[2], GREENFIELD Charles M., HYATT Alan W., La HAYE Robert J., LAO Lang L., LAZARUS Ed A.[3], MAKOWSKI Mike A.[4], MURAKAMI Masanori[3], PETTY Clinton C., PINSKER Robert I., RICE Brad W.[4], STRAIT Edward J., WADE Mickey R.[3] and WATKINS Jon G.[5]

General Atomics, P.O. Box 85608, San Diego, California 92186-5608

[1]University of Texas, Austin, Texas

[2]Columbia University, New York, New York

[3]Oak Ridge National Laboratory, Oak Ridge, Tennessee

[4]Lawrence Livermore National Laboratory, Livermore, California

[5]Sandia National Laboratory, Albuquerque, New Mexico

(Received: 18 January 2000 / Accepted: 13 July 2000)

Abstract

A major portion of the research program of the DIII-D tokamak collaboration is devoted to the development and demonstration of high performance advanced tokamak plasmas, with profiles as close as possible to those anticipated for steady-state operation. The work during the 1999 campaign has resulted in significant progress toward this goal. High normalized performance ($\beta_N \sim 4$ and $\beta_N H89 \sim 9$) discharges have been sustained for up to 2 s. These plasmas are in H-mode with rapid ELMs. The most common limiting phenomena are resistive wall modes (RWMs) rather than neoclassical tearing modes (NTMs). NTMs do occur, apparently triggered by the RWMs. The observed pressure is well above the calculated beta limit without a wall, and $\beta_N > 4\ \ell_i$ throughout the high performance phase. The bootstrap current is estimated to be > 50% of the total, and measurements of the internal loop voltage show that only about 25% of the current is inductively driven. The central q profile is flat, as is the calculated bootstrap current profile, due to the absence of any localized pressure gradients. The residual inductive current is localized around $r/a \sim 0.5$. To demonstrate quasi-stationary operation, it will be necessary to replace the residual inductive current with ECCD at the same minor radius. To effectively apply ECH and ECCD to these discharges, density control will be needed. Preliminary experiments using the DIII-D cryopump have reduced the density by ~20%. A new EC power system and a new private flux cryopump will be available for the 2000 campaign.

Keywords:

DIII-D, advanced tokamak, tokamak, MHD stability, steady-state

1. Introduction

A major focus of the DIII-D program is to develop the scientific basis for tokamak optimization, and to develop and demonstrate a high performance, steady-state tokamak operating regime. This is motivated by the benefits that accrue from steady-state operation of any magnetic confinement fusion reactor. For a tokamak,

*Corresponding author's e-mail: politzer@fusion.gat.com

©2000 by The Japan Society of Plasma Science and Nuclear Fusion Research

steady-state implies close to 100% bootstrap fraction (f_{bs}), otherwise the power needed for noninductive current drive would be unaffordable. To get high f_{bs} while maintaining high fusion power density and wall loading (i.e., high β) requires operation at low rotational transform (moderate q) with increased values of normalized beta ($\beta_N \propto p/IB$) and confinement (e.g., $H_{89} = \tau_E/\tau_{ITER89P}$). For example, a reactor with an operating point at $\beta_N H \approx 5$ and $q \approx 3$ with $f_{bs} \approx 40\%$ will need to reach $\beta_N H \approx 12.5$ at $q \approx 4.7$ to get $f_{bs} \approx 100\%$.

The near-term goal for the DIII-D program is to obtain normalized performance double that of conventional ELMy H-mode or $\beta_N H_{89} \geq 10$. In addition, the plasma current should be fully noninductive, with a relaxed loop voltage profile and >50% bootstrap fraction.

This paper describes recent progress toward this goal. The MHD phenomena which limit the initial rise of the plasma energy, maintain an apparently stationary state, and eventually cause the discharge to lose energy will be discussed. It is an indication of the success of the plasma optimization efforts that we are reaching several limiting conditions simultaneously. The key obstacle is continual evolution of the current profile toward a less stable configuration. The coming campaign will make use of new tools to maintain a steady, noninductive current profile.

2. Producing Optimum Plasma Conditions

The near-term scenario for an optimized plasma in DIII-D has been developed to maximize stability to ballooning modes and to low-n kink modes. The desired q profile has a minimum value just above 2, located near the half-radius. The elevated q helps to enhance the bootstrap current density and eliminates the sawtooth instability. The inner region has weak negative shear – to provide stability to ballooning and neoclassical tearing modes and to assist confinement improvement through stabilization of turbulence by increased shear in the E × B flow. Note that strong negative shear in the central region can lead to destabilization of resistive interchange modes. The outer region has strong positive shear which improves the stability of the neoclassical tearing modes (NTMs).

One of the best performing DIII-D plasmas from the recent campaign is shown in Fig. 1. This plasma has $B = 1.6$ T, and a flat-top plasma current $I = 1.2$ MA. The maximum injected neutral beam power is 11 MW. This discharge has $\beta_N H_{89} > 9$, sustained for 2 s, which is 16 τ_E or about one current profile relaxation time. The

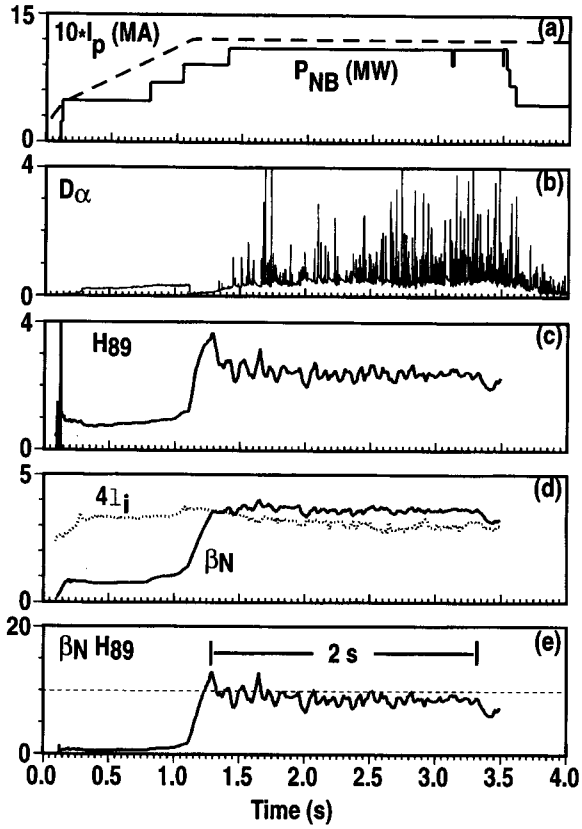

Fig. 1 DIII-D discharge 98977 parameters versus time. (a) plasma current and NB power; (b) Dα signal indicating L-H transition and ELMy H-mode phase; (c) energy confinement time normalized to the ITER89P scaling; (d) normalized beta compared to 4 × the internal inductance; (e) combined figure of merit.

formation of the discharge follows the now-standard recipe of starting NBI early in the current ramp-up, in order to produce a high and inverted q profile [1]. The timing of the transition from L-mode to H-mode is controlled by small changes in the plasma shape, from a single null biased against the ∇B drift direction to a balanced double null.

The ELM-free period ends with the appearance of small ELMs which reduce the confinement but which do not cause a drastic loss in energy content. This is in distinction to many earlier experiments in which a high performance ELM-free phase ended with large amplitude ELMs or a global mode, leading to a significant reduction in stored energy [2]. This discharge maintains stationary conditions of global confinement and β, although the current profile continues to evolve. The repeated small decreases in β_N and H_{89}, including

the one at 3.3 s, are associated with low amplitude resistive wall modes.

3. Beta Saturation

The rapid pressure rise during the ELM-free phase ends before the first ELM occurs. An expanded view of this period of a similar discharge is shown in Fig. 2.

At the L-H transition, the confinement improvement leads to a large increase in $d\beta/dt$. At approximately 1.275 s, a high frequency instability appears. Associated with this instability is a drop to zero in $d\beta/dt$. The instability disappears at the first ELM (1.332 s), but recurs in a bursting fashion throughout the discharge. These bursts are broadband in frequency, 100–200 kHz and have a medium toroidal mode number ($n \approx 5$–9). Their behavior is consistent with Alfvénic modes driven by the fast ion pressure. The appearance of these modes does not correlate with the thermal plasma β or with the value of q. The coupling of these modes to the fast ion population in the plasma core may cause a spatial redistribution of the fast ions to the edge region. Thus these modes can limit the power delivered to the core plasma.

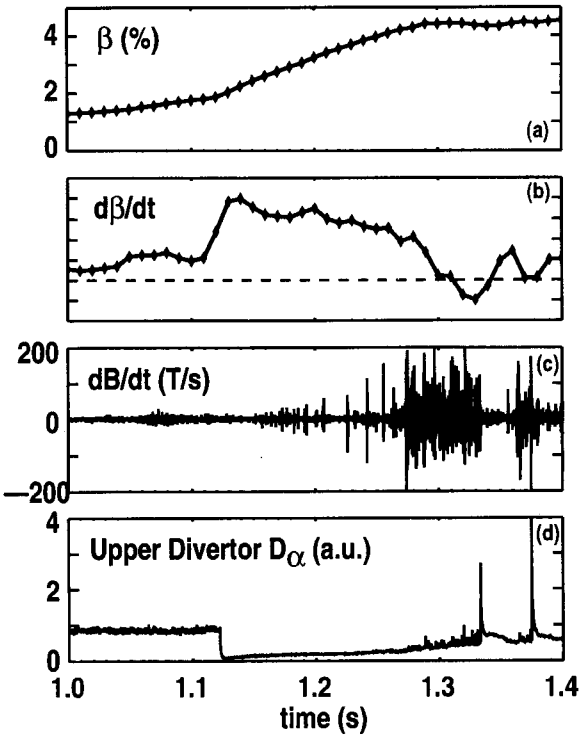

Fig. 2 Increase of beta after L-H transition at 1.12 s in discharge 99505 and beta saturation associated with high frequency burst.

In addition to the ELMs and fast-ion instabilities, resistive wall modes (RWMs) play a role in limiting the β during the quasi-steady portion of these discharges [3]. Many discharges show the phenomena illustrated in Fig. 3.

A slowly rotating n = 1 mode comes and goes during the quasi-stationary phase. The real frequency is below 100 Hz, consistent with the resistive wall time rather than the plasma rotation rate; the growth rate is similar to the real frequency. These modes appear when β is at or above the stability limit without a wall. The no-wall limit is in the neighborhood of $\beta_N \geq 4\,\ell_i$ [4]. As the amplitude rises, β drops and the plasma rotation slows. If the mode is quenched, β again rises. The high performance phase of the discharge is often terminated when an RWM grows to large amplitude instead of quenching. The RWM growth is associated with a large decrease in the toroidal rotation rate of the plasma. A hypothesis for why the RWM sometimes quenches and sometimes causes a β collapse is based on the relative reduction of β and rotation during the mode growth [5].

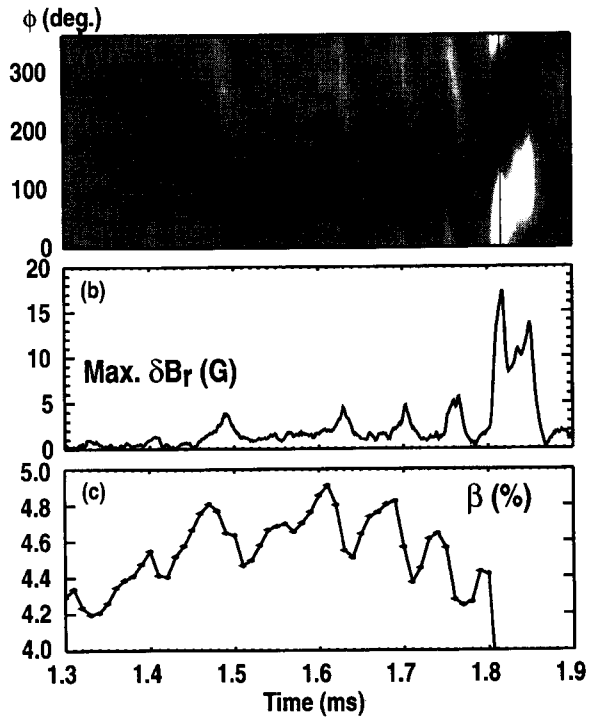

Fig. 3 Repeated appearance and quenching of RWM, followed by RWM growth to large amplitude and collapse of beta in discharge 98526. The first frame (a) is a contour plot of δB_r measured by saddle coils outside the vessel as a function of time and toroidal angle.

If the β is reduced below the no-wall limit while there is still sufficient rotation, the mode quenches. If the rotation has been reduced to too low a level, the plasma cannot recover and the RWM continues to grow.

4. Profile Evolution and Control Requirements

In these discharges, the desired current profile is formed using the interaction of the current ramp-up, neutral beam power programming, and control of the L-H transition. The current density is peaked at about the half-radius and is low at the edge. The subsequent evolution of these profiles, as well as density and temperature is shown in Fig. 4.

The J and q profiles are very similar in the L-mode and early H-mode phases. As the H-mode progresses, the current peak diffuses toward the axis, and the edge J rises. The q profile evolves such that the minimum value decreases and moves toward the axis. The shear in the outer region decreases. The increase in J near the edge increases the instability drive for RWMs. The reduction in magnetic shear increases the likelihood of the neoclassical tearing mode instability, particularly at the $q = 2$ and $q = 5/2$ surfaces.

The density increases across the plasma at the L-H transition and continues to rise during the discharge. The increasing H-mode pedestal at the edge causes a peak in the bootstrap current, which leads to the rise in J near the edge. The ion temperature shows evidence of better confinement in the central region than near the edge throughout the discharge. The temperature also jumps up at the L-H transition, but subsequently falls as the density rises, maintaining constant β.

Fig. 5 illustrates the components of the current profile during the ELMy H-mode phase. The bootstrap current density is flat across most of the plasma, with a peak at the edge due to the H-mode pedestal. In this case, $f_{bs} \approx 50\%$. The current density generated by the neutral beams is strongly peaked at the center, and accounts for an additional 25% of the total current. The inductive current density provides the remaining 25% of the total. It is peaked at about the half radius.

This analysis indicates what is needed to maintain a stationary profile. An additional current source is needed to replace the inductive current at the half-radius. In DIII-D, the electron cyclotron current drive system has been chosen because it provides the needed localization and controllability [7]. We are presently installing a 110 GHz gyrotron system which can deliver ≥ 2.3 MW to the plasma.

In order to obtain the required current, it is necessary to prevent the density increase during the discharge. This will be done with the newly expanded DIII-D pump and baffle system, which now provides a

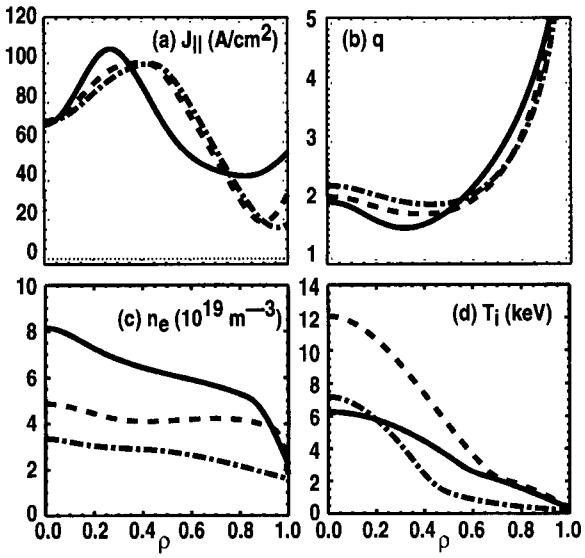

Fig. 4 Profiles of (a) current density, (b) q, (c) electron density, and (d) ion temperature in discharge 98549. TImes are in L-mode (1.11 s, dot-dash line), early in H-mode (1.26 s, dash line), and late in H-mode (1.50 s, solid line).

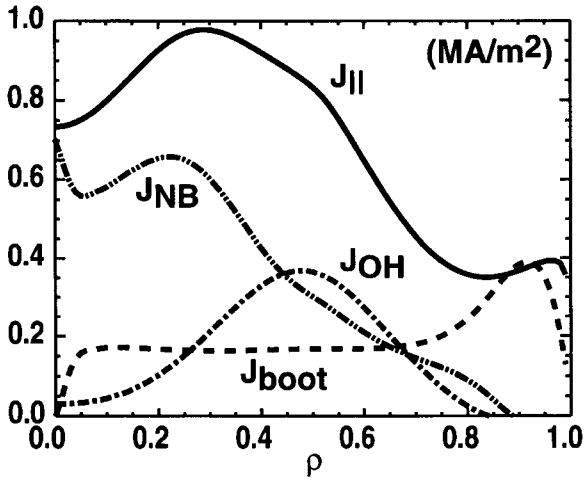

Fig. 5 Components of the current profile in discharge 98549 at 1600 ms. The total parallel current density is determined from the equilibrium reconstruction; the Ohmic current is from the time derivative of the poloidal flux and the neoclassical conductivity [6]; the bootstrap current is the neoclassical value [6]; the difference $J_{\|} - J_{OH} - J_{boot}$ is attributed to the neutral beam driven current.

more tightly baffled region around one of the x-points, with cryopumps on the outer separatrix leg and in the private flux region [8]. Experiments done in the past year with a single pump have achieved a reduction of about 20% in the average density.

5. Summary

Good progress has been made toward the DIII-D project goal of demonstrating a steady-state plasma with a relaxed, fully noninductive current profile, and a normalized performance twice that of standard tokamak H-mode. A discharge with 75% noninductive current has been sustained at $\beta_N H_{89} \geq 9$ for 2 s or 16 energy confinement times. The effort in the coming year will be devoted to gaining a better understanding of the processes that limit this performance. With the new tools for pumping and ECCD, we should be able to reach the goal of a stationary, fully noninductive plasma. Other efforts now under way in the DIII-D program will also contribute to the steady-state, high performance objective over the next two years. We are studying the physics of NTMs, RWMs, transport barriers, and the H-mode edge pedestal, and are applying new understanding to developing active control of these phenomena.

Acknowledgements

This work was supported by the U.S. Department of Energy under Contracts Nos. DE-AC03-99ER54463, DE-AC05-96OR22464, W-7405-ENG-48, DE-AC04-94AL85000, and Grants Nos. DE-FG03-97ER54415 and DE-FG02-98ER53297.

References

[1] B.W. Rice *et al.*, Plasma Phys. Control Fusion **38**, 869 (1966).
[2] L.L. Lao *et al.*, Nucl. Fusion **39**, 1785 (1999).
[3] A.M. Garofalo *et al.*, Phys. Plasmas **6**, 1893 (1999); A.M. Garofalo *et al.*, Phys. Rev. Lett. **82**, 3811 (1999).
[4] E.J. Strait, Phys. Plasmas **4**, 1783 (1997).
[5] A.M. Garofalo *et al.*, Bull. Am. Phys. Soc. **44**, 129 (1999).
[6] O. Sauter *et al.*, Phys. Plasmas **6**, 2834 (1999).
[7] T.C. Luce *et al.*, Phys. Rev. Lett. **83**, 4550 (1999).
[8] M.A. Mahdavi *et al.*, J. Nucl. Mater. **13**, 222 (1995).